Available online at www.sciencedirect.com
SCIENCE DIRECT
Global and Planetary Change 47 (2005) 17–35
GLOBAL AND PLANETARY CHANGE
www.elsevier.com/locate/gloplacha

Impact of millennial-scale Holocene climate variability on eastern North American terrestrial ecosystems: pollen-based climatic reconstruction

Debra A. Willard[a,*], Christopher E. Bernhardt[a], David A. Korejwo[a], Stephen R. Meyers[b]

[a]U.S. Geological Survey, 926A National Center, 12201 Sunrise Valley Drive, Reston, VA 20192, United States
[b]Geology and Geophysics Department, Yale University, P.O. Box 208109, New Haven, CT, 06520-8109, United States

Received 17 March 2004; accepted 30 November 2004

Abstract

We present paleoclimatic evidence for a series of Holocene millennial-scale cool intervals in eastern North America that occurred every ~1400 years and lasted ~300–500 years, based on pollen data from Chesapeake Bay in the mid-Atlantic region of the United States. The cool events are indicated by significant decreases in pine pollen, which we interpret as representing decreases in January temperatures of between 0.2° and 2 °C. These temperature decreases include excursions during the Little Ice Age (~1300–1600 AD) and the 8 ka cold event. The timing of the pine minima is correlated with a series of quasi-periodic cold intervals documented by various proxies in Greenland, North Atlantic, and Alaskan cores and with solar minima interpreted from cosmogenic isotope records. These events may represent changes in circumpolar vortex size and configuration in response to intervals of decreased solar activity, which altered jet stream patterns to enhance meridional circulation over eastern North America.

Keywords: Paleoclimatology; Holocene; Little Ice Age; Chesapeake Bay; pollen

1. Introduction

Debates on the causes of millennial-scale climate variability during an interglacial have included solar forcing, internally forced changes in deep oceanic circulation, and modulations of atmospheric circulation such as the North Atlantic Oscillation (Bond et al., 2001; Keigwin and Pickart, 1999; Mayewski et al., 1997; Shindell et al., 2001). Such variability has been documented in Holocene records of drift ice in the North Atlantic Ocean (Bond et al., 2001), $\delta^{18}O$ in Irish speleothems and Greenland ice cores (Johnsen et al., 2001; McDermott et al., 2001), sea-surface temperatures in the subtropical southeastern Atlantic

* Corresponding author. Tel.: +1 703 648 5320; fax: +1 703 648 6953.
E-mail address: dwillard@usgs.gov (D.A. Willard).

0921-8181/$ - see front matter © 2004 Elsevier B.V. All rights reserved.
doi:10.1016/j.gloplacha.2004.11.017

Ocean (deMenocal et al., 2000), and biogenic silica and pollen records from Alaskan lakes (Hu et al., 2003). Given recent concerns regarding the impact of anthropogenic greenhouse gases on global climate, this broad-scale signal of quasi-periodic (1500±500 years) climate forcing needs to be understood in the context of its influence on natural trends in global temperatures, precipitation, and sea-ice extent over the next few centuries. Because climate response to external forcing factors may not be globally uniform or synchronous and because feedbacks exist among different forcing factors, it is important to develop an understanding of their relative roles in driving climate periodicity. To do so, examination of high-resolution paleoclimate records from different regions and ecosystems is critical. Thus far, Holocene records clearly documenting millennial-scale climate variability have been confined primarily to marine, ice core, and high-latitude lacustrine sites; no Holocene records have been available from mid-latitude terrestrial sites in the eastern United States with sufficient temporal resolution to examine millennial-scale varibiality.

In this paper, we present high-resolution sediment records from Chesapeake Bay, which detail the impact of Holocene climate variability on terrestrial and estuarine ecosystems in a key climatic region of North America. Chesapeake Bay is the largest estuary in the United States, extending >300 km in length, covering an area of 6500 km^2, and draining a watershed of 166,000 km^2 (Fig. 1). The bay formed when rapid sea-level rise between ~8.0 and 7.6 ka flooded the paleo-Susquehanna River system (Cronin et al., 2003; Hobbs, 2004), abruptly changing the fluvial system to an estuary. Chesapeake Bay has a deep (20–50 m) channel formed by the Susquehanna River during sea-level lowstands of the last glacial period and a thick (10 to >20 m) Holocene sequence identified by geophysical surveys (Colman and Halka, 1989; Halka et al., 2000; Vogt et al., 2000). Pre-Colonial Holocene sedimentation rates of 0.2–1.0 cm $year^{-1}$ provide a stratigraphic record of paleoclimatic variability with temporal resolution that exceeds most lacustrine and marine records. This record includes an almost complete Holocene record and abundant floral (Willard et al., 2003), faunal (Cronin et al., 2000, 2003), and geochemical (Zimmerman and Canuel, 2000) proxies to evaluate ecosystem response to climatic fluctuations on a variety of temporal scales.

Chesapeake Bay lies within the Atlantic Coastal Plain and is surrounded by oak–pine forests in the southern two-thirds of the bay (south of ~38°N latitude); oak–chestnut and tulip poplar forests dominate along the northern reaches of the bay (Braun, 1950; Brush et al., 1980; Greller, 1988). The boundary between the two forest types corresponds to changes in substrate type, drainage potential of the native soils, and climatic regime. Oak–pine forests occupy unconsolidated sediments with low topographic relief in the coastal plain; deciduous forests occupy drier sites with greater topographic relief to the north. South of the Chesapeake Bay mouth, pines become progressively more abundant and grade into the southeastern pine forests (Braun, 1950; Greller, 1988).

A climatic transition zone delineated by the position of the polar jet stream crosses Chesapeake Bay, and changes in its position directly influence regional temperature, precipitation, and storm frequency and intensity (Vega et al., 1998, 1999). The position of the jet stream generally reflects the shape and size of the circumpolar vortex, which incorporates atmospheric circulation patterns in both eastern and western hemispheres. During times of meridional circulation, the jet stream exhibits an enhanced ridge and trough configuration, whereas a flattened jet stream characterizes intervals of zonal circulation. In the eastern United States, intervals of enhanced meridional flow, such as occurred between 1966 and 1990, result in the advection of polar air south, cooler temperatures, and increased cyclone frequency (Davis and Benkovic, 1992). The impact of relatively subtle shifts in jet stream position on temperature and precipitation in the mid-Atlantic region makes Chesapeake Bay an ideal site for paleoclimate studies.

The possible influence of solar variability on atmospheric circulation patterns and the earth's climate recently has been explored through analysis of satellite monitoring data, which have a limited period of record from the mid-1940s to the present (Angell, 1992; Davis and Benkovic, 1992), and using historical compilations of sun spot records, which extend observational records to 2000 years BP (Pang and Yau, 2002). These studies show correlations between solar cycles, circumpolar vortex configuration, and various atmospheric circulation patterns (i.e., El Niño,

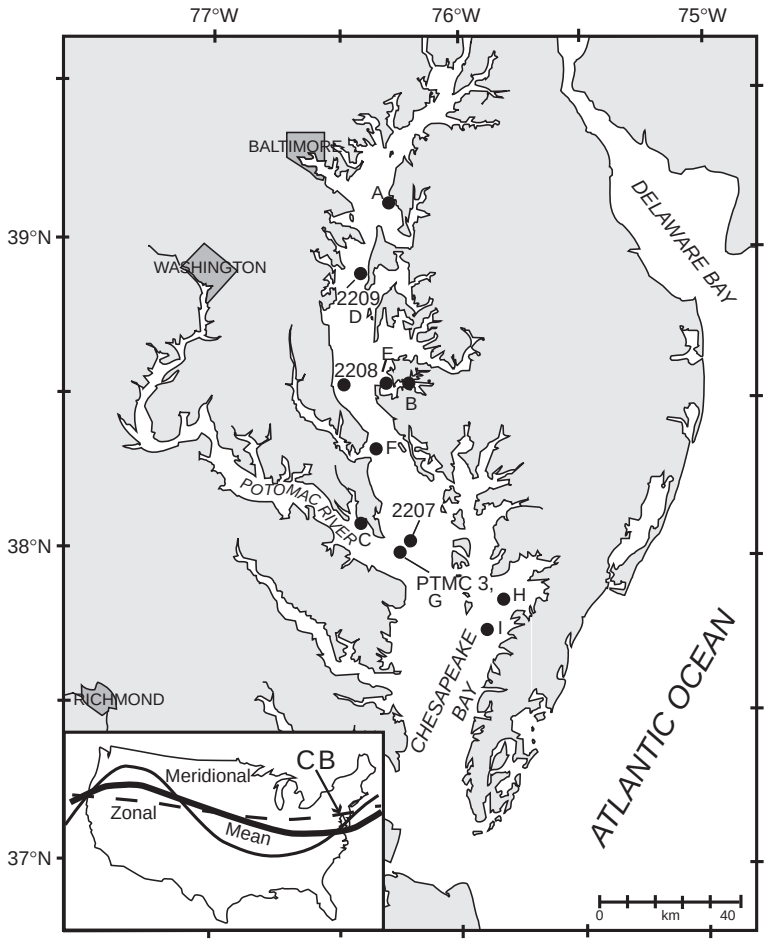

Fig. 1. Location of coring sites in Chesapeake Bay (CB) in eastern North America. Core sites include MD99-2207, MD99-2208, MD99-2209, and PTMC3-2. Lettered circles indicate collection sites for samples used to test validity of 400-year marine correction for ^{14}C dates. Circles A–C represent location of modern oyster samples (Colman et al., 2002); circles D–I represent location of cores in which shells from post-Colonial samples were radiocarbon dated in this study (see text for explanation). Inset map shows position of Chesapeake Bay on eastern coast of North America, a simplified illustration of the mean position of the polar jet stream (thick line), and its altered configuration during zonal (dashed line) and meridional (thin line) flow regimes.

quasi-biennial oscillation) over decadal to centennial time scales (Angell, 1998; Shindell et al., 2001). Although only a few mechanisms for solar control on atmospheric circulation patterns have been proposed (i.e., Tinsley, 2000), the apparent correlations support earlier hypotheses that the size and intensity of the vortex, perhaps influenced by solar variability, may have governed much post-Glacial climate variability on centennial to millennial time scales (Willett, 1949). The decadal- to centennial-scale resolution of the Chesapeake Bay sedimentary record provides an opportunity to evaluate the impact of such variability on a terrestrial mid-latitude record. Pollen is well preserved throughout the sediments, and calibration of pollen assemblages from surface sediments with plant assemblages in adjacent forests along the east coast facilitates interpretation of changes in forest composition, temperature, and precipitation.

2. Calibration of pollen and climatic data

Pollen assemblages preserved in sediments from North American estuaries and the western Atlantic

Ocean shelf provide a regional record of vegetation on the adjacent coasts because the prevailing westerly breezes during the flowering season deposit pollen abundantly in shallow marine and estuarine sediments (Mudie, 1980, 1982; Litwin and Andrle, 1992; Willard, 1994). To assess the correlation between abundance of pollen from dominant wind-pollinated taxa in the region and climatic parameters, we compared *Pinus* and *Quercus* pollen abundance in estuarine and shallow marine (≤100 m) sediments from the western Atlantic Ocean (Emery, 1966) with latitude, mean January temperature, and mean annual precipitation from the nearest climate monitoring stations. Climatic data were averaged over the years 1971–2000 (NCDC, 2000). Pollen data were obtained from Buening et al. (2000), Litwin and Andrle (1992), Edwards and Willard (2001) and Willard (new data available online at the North American Pollen Database (NAPD) at the World Data Center for Paleoclimatology in Boulder, CO: http://www.ngdc.noaa.gov/paleo/pollen.html).

Abundance of *Pinus* pollen in modern sediments shows a clear south to north gradient of high to low percent abundance (Fig. 2A), ranging from >80% at 28°N to <20% at 42°N. This gradient mirrors the abundance of southern pines (*Pinus echinata*, *Pinus elliottii*, *Pinus palustris*, *Pinus taeda*, *Pinus virginiana*) in eastern United States forests. Their approximate northern limit is ~38°N (Bartlein et al., 1986); measurements of current timber stock indicate that southeastern states (Virginia to Florida) contain a combined stock of 45,147 million cubic feet (mcf) of southern pines, compared to 1493 mcf from Maryland through the New England states (Smith et al., 1997). These pine species require warm winters (>−0.6 °C), high moisture availability (>885 mm annual precipitation), and unconsolidated soils (Iverson et al., 1999; Thompson et al., 2000). *Quercus* pollen abundance shows no correlation with latitude or climatic parameters (r^2<0.011), which is consistent with their common distribution throughout eastern North American forests.

Pinus pollen abundance and mean January temperatures are strongly correlated (r^2=0.91; Fig. 2B), providing a proxy for winter temperature fluctuations. The much weaker correlation between *Pinus* pollen abundance and mean annual precipitation (r^2=0.331) reflects the lack of a strong latitudinal precipitation

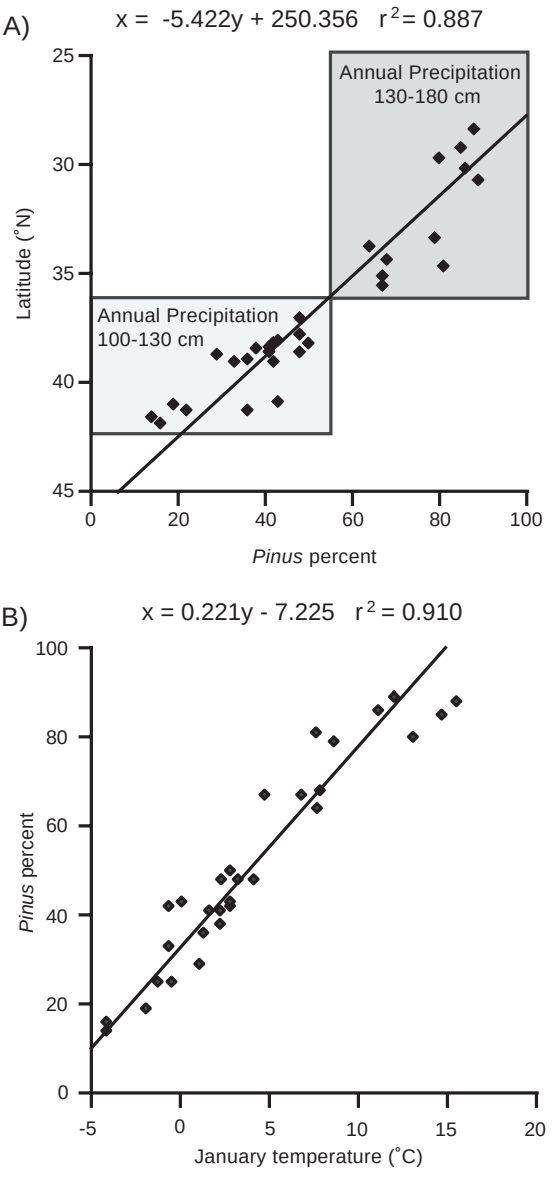

Fig. 2. (A) Regression model (r^2=0.887) for *Pinus* pollen abundance in estuarine and shallow marine sediments of the western Atlantic Ocean vs. latitude. (B) Regression model (r^2=0.910) for *Pinus* pollen abundance in estuarine and shallow marine sediments of the western Atlantic Ocean vs. January temperature. Pollen data compiled from Buening et al. (2000), Edwards and Willard (2001), Litwin and Andrle (1992), and Willard (new data available on North American Pollen Database: http://www.ngdc.noaa.gov/paleo/pollen.html). Climate data were taken from nearest weather stations and averaged over the years 1971–2000 (National Climate Data Center, 2000).

gradient. However, samples collected north of 37° latitude were comprised of <50% *Pinus* pollen, and those sites receive an average of 100–130 cm annual precipitation, whereas those collected south of 36°N are characterized by >65% *Pinus* pollen and receive 130–180 cm annual precipitation (Fig. 2A). This relationship is consistent with data on *Pinus* pollen production rates in the Washington, DC region, which covary with precipitation of the previous year. Over an 11-year period, comparison of atmospheric pollen concentrations with June to December precipitation (when cone production occurs) indicates that precipitation during that period explains more than one-third of the variation in atmospheric *Pinus* pollen abundance. When precipitation is greatest, atmospheric *Pinus* pollen concentrations are greatest (Willard et al., 2003). Therefore, we use *Pinus* pollen abundance as a proxy for both winter temperature and mean annual precipitation. Using only the relationship between pollen abundance and winter temperature derived above, a 20% increase in pine pollen in estuarine and shallow-marine sediments is equivalent to an increase in January temperature of ~4.5 °C (Fig. 2B). However, because of the combined influences of winter temperature and precipitation, it is likely that temperature reconstructions based only on the pine–temperature correlation overestimate absolute temperature variability to some extent.

3. Holocene pollen record from Chesapeake Bay sediment cores

3.1. Stratigraphy and age

The Holocene vegetational history presented herein is based on pollen assemblages from four sediment cores collected in the mainstem of Chesapeake Bay (Fig. 1). We used a modified Calypso corer on the IMAGES V cruise of the R/V *Marion Dufresne* to collect three cores in 1999: MD99-2207 (38°01.83′N, 76°12.88′W, 2070 cm long, 25 m water depth [mwd]); MD99-2208 (38°32.24′N, 76°29.19′W, 782 cm long, 10 mwd); and MD99-2209 (38°53.18′N, 76°23.68′W, 1720 cm long, 26 mwd). We collected a shorter piston core (PTMC3-2, 38°01.6118′N, 76°13.1938′W, 414 cm long, 23.1 mwd) on the R/V *Kerhin* in 1996.

Forty-three accelerator mass spectrometer (AMS) radiocarbon dates (all dates are presented as calibrated years before present) (Table 1) and well-documented biostratigraphic events from numerous eastern North American sites form the basis for age models for these cores. Age models for each core were determined by a combination of linear interpolation and best-fit polynomials between radiocarbon dates obtained on molluskan shells and foraminifera, calibrated with the marine reservoir correction of 400 years (Fig. 3). Use of the marine correction is based on analyses of oysters collected live in Chesapeake Bay before atmospheric nuclear testing and shells from sediment cores collected within the zone identified as 1880–1910 AD based on pollen biostratigraphy. The oyster shells yielded an average reservoir correction of 365±143 years (Colman et al., 2002). We also identified intervals in six sediment cores collected south of the estuarine turbidity maximum that represent the interval of peak land clearance in the watershed (1880–1910 AD) using the abundance of ragweed (*Ambrosia*) pollen (after Willard et al., 2003). Shells of *Mulinia*, an unidentified mollusk, and the bryozoan *Haminoea solitaria* were collected from the interval and dated using AMS (Table 2). The mean reservoir effect from these 10 samples is 374.5±60 years, also comparable to the marine correction. These data indicate that the standard marine reservoir correction of 400 years is appropriate for use in Chesapeake Bay sites south of the estuarine turbidity maximum.

The basal date of 10.5 ka in core MD99-2207 is based on percent abundance of pine (*Pinus*) and oak (*Quercus*) (23% and 53%, respectively). Such high abundances in eastern North American pollen assemblages were not attained until at least 10.5 cal ka (Kneller and Peteet, 1993; Watts, 1979); therefore, this is a conservative estimate, and basal sediments may be younger. Confirmation of this estimate is provided by comparison of paleomagnetic inclination data from MD99-2207 with the composite inclination curve from the northeastern United States, which places the base of the core at 10–10.5 ka (Clifford Heil, personal communication, 2003). The *Carya* increase abundance from <2% to >4% at 1300–1250 cm in MD99-2207 correlates with an increase at ~9.4 ka documented in mid-Atlantic ponds and bogs (Watts, 1979) and is within the error range of the radiocarbon date of 9.21 (9.63–9.04) ka at 1250 cm.

Table 1
Locality, water depth, and age information for cores MD99-2209, PRCK 1-2, PTXT 2-P-5, and PTMC 3-P-2

Site and core no.	Latitude (°N)	Longitude (°W)	Water Depth (m)	Lab #	Depth of ^{14}C date (cm)	Material dated	$\delta^{13}C$	^{14}C age (conventional)	1σ[a]	Calibrated age (years BP)	$\pm 2\sigma$[b] (years BP)
Rhode River											
MD99-2209	38°53.18′	76°23.68′	26	OS-21226	296	bivalve	−0.87	610	30	270	300–150
RD 98-1[c]	38°53.202′	76°23.502′	26.5	OS-19215	340	bivalve	−0.87	725	55	340	270–460
MD99-2209	38°53.18′	76°23.68′	26	OS-21381	369	bivalve	−0.57	745	35	410	450–510
MD99-2209	38°53.18′	76°23.68′	26	OS-21382	455	bivalve	−0.68	1150	40	680	760–640
RD 98-1[c]	38°53.202′	76°23.502′	26.5	OS-19214	457	bivalve	−1.03	1150	85	675	550–870
MD99-2209	38°53.18′	76°23.68′	26	OS-21227	485	bivalve	−1.29	1240	30	770	870–710
MD99-2209	38°53.18′	76°23.68′	26	OS-21383	576	bivalve	−0.9	1600	35	1165	1230–1070
MD99-2209	38°53.18′	76°23.68′	26	OS-21384	665	bivalve	−1.73	2050	40	1610	1700–1520
MD99-2209	38°53.18′	76°23.68′	26	OS-21228	733	bivalve	−0.77	2210	35	1810	1880–1720
MD99-2209	38°53.18′	76°23.68′	26	OS-21229	780	bivalve	−0.74	2500	35	2140	2280–2070
MD99-2209	38°53.18′	76°23.68′	26	OS-21385	820	bivalve	−0.18	4230	40	4340	4210–4420
MD99-2209	38°53.18′	76°23.68′	26	OS-21230	904	bivalve	−0.7	5530	40	5905	5810–5990
MD99-2209	38°53.18′	76°23.68′	26	OS-21231	1029.5	bivalve	−0.14	5690	40	6100	5980–6180
MD99-2209	38°53.18′	76°23.68′	26	OS-21232	1159	bivalve	−0.08	5690	40	6380	6290–6440
MD99-2209	38°53.18′	76°23.68′	26	OS-21233	1199	bivalve	0.02	5980	40	6390	6300–6460
MD99-2209	38°53.18′	76°23.68′	26	OS-21488	1439	bivalve	−0.74	6250	35	6700	6620–6770
MD99-2209	38°53.18′	76°23.68′	26	OS-21386	1605	bivalve	−3.73	6290	35	6730	6650–6830
MD99-2209	38°53.18′	76°23.68′	26	OS-21489	1694	bivalve	−3.53	8670	45	9220	9050–9660
MD99-2209	38°53.18′	76°23.68′	26	OS-21387	1694	oyster	−1.04	6660	45	7200	7080–7280
MD99-2209	38°53.18′	76°23.68′	26	OS-21388	1705	bivalve	−1.49	7050	40	7550	7450–7593
MD99-2209	38°53.18′	76°23.68′	26	OS-21389	1720	bivalve	−1.5	7100	45	7570	7500–7650
Parker Creek											
MD99-2208	38°32.2400′	76°29.1900′	10	WW 3392	59	mollusk	0	670	40	297	258–414
MD99-2208	38°32.2400′	76°29.1900′	10	WW-3393	559	bivalve	−3	5080	40	5447	5317–5536
MD99-2208	38°32.2400′	76°29.1900′	10	WW-2705	629	bivalve	0	6055	65	6462	6307–6632
MD99-2208	38°32.2400′	76°29.1900′	10	WW-3395	751.5	oyster	−4.6	6980	40	7410	7316–7465
MD99-2208	38°32.2400′	76°29.1900′	10	WW-3396	765	oyster	−5.7	7360	40	7810	7721–7915

MD99-2208	38°32.2400′	76°29.1900′	10	WW-3397	779	oyster	−8.7	7780	40	8217	8151–8336
MD99-2208	38°32.2400′	76°29.1900′	10	WW-2706	779	oyster	−5.6	7740	80	8177	8004–8360
Potomac River											
PTMC 3-P-2	38°01.6118′	76°13.1938′	23.1	OS 15679	81	*Mulinia lateralis*	0.01	540	30	150	0–260
PTMC 3-P-2	38°01.6118′	76°13.1938′	23.1	WW 1284	141	*Mulinia lateralis*	0.1	540	50	150	0–280
PTMC 3-P-2	38°01.6118′	76°13.1938′	23.1	OS 15680	161	*Mulinia lateralis*	−0.29	885	35	500	450–540
PTMC 3-P-2	38°01.6118′	76°13.1938′	23.1	OS 15681	211	*Mulinia lateralis*	0.01	1150	25	675	650–720
PTMC 3-P-2	38°01.6118′	76°13.1938′	23.1	WW 1589	225	*Mulinia lateralis*	0	990	40	550	510–640
PTMC 3-P-2	38°01.6118′	76°13.1938′	23.1	IS 17242	229	*Elphidium*	−1.72	1230	30	750	680–830
PTMC 3-P-2	38°01.6118′	76°13.1938′	23.1	OS 15689	297	*Mulinia lateralis*	0.1	1530	70	1060	920–1230
PTMC 3-P-2	38°01.6118′	76°13.1938′	23.1	OS 17508	331	*Elphidium*	−2.41*	2450	256	2080	1530–2710
MD99-2207	38°01.8300′	76°12.880′	25	OS-21487	221.5	bivalve	−0.42	855	25	490	450–510
MD99-2207	38°01.8300′	76°12.880′	25	OS-25825	377.5	bivalve	−2.04*	125	50	0	–
MD99-2207	38°01.8300′	76°12.880′	25	OS-21670	387.5	bivalve	0.11	4100	45	4140	4000–4270
MD99-2207	38°01.8300′	76°12.880′	25	OS-21671	573.5	bivalve	−0.13	4470	45	4630	4530–4790
MD99-2207	38°01.8300′	76°12.880′	25	OS-25826	687.5	bivalve	0.14	4590	55	4810	4630–4930
MD99-2207	38°01.8300′	76°12.880′	25	OS-21664	777	bivalve	0.2	6130	55	6560	6420–6670
MD99-2207	38°01.8300′	76°12.880′	25	OS-21665	833.5	bivalve	0.18	6430	65	6900	6740–7080
MD99-2207	38°01.8300′	76°12.880′	25	OS-21666	901	bivalve	−8.09*	9150	65	9810	9530–10,090
MD99-2207	38°01.8300′	76°12.880′	25	OS-25827	901	bivalve	0.7	6540	45	7025	6930–7160
MD99-2207	38°01.8300′	76°12.880′	25	OS-25828	960	bivalve	−1.94*	8150	55	8600	8470–8850
MD99-2207	38°01.8300′	76°12.880′	25	OS-21667	993	bivalve	0.37	7080	60	7560	7450–7650
MD99-2207	38°01.8300′	76°12.880′	25	OS-25829	1152.5	bivalve	−7.27*	8930	65	9475	9100–9820
MD99-2207	38°01.8300′	76°12.880′	25	OS-21668	1161	bivalve	−9.66*	9400	100	10,130	9710–10,560
MD99-2207	38°01.8300′	76°12.880′	25	OS-21503	2051	wood	−27.78*	10,400	45	12,340	11,950–12,800
MD99-2207	38°01.8300′	76°12.880′	25	B-160832	1045	non-marine mollusc	−9.5*	9440	60	7894	7434–7964
MD99-2207	38°01.8300′	76°12.880′	25	B-106833	1090	non-marine mollusc	−9*	9220	40	8191	8041–8311
MD99-2207	38°01.8300′	76°12.880′	25	B-106834	1249	bivalve	−1.6	8800	40	9210	9040–9630

Radiocarbon dates compiled from Cronin et al. (2000, 2003) and Colman et al. (2002). Dates marked with an asterisk were not used in age models because $\delta^{13}C$ values suggested transport or reworking from adjacent units or because they represent reversals.

[a] One-sigma counting errors.

[b] Upper and lower limits of range based on two-sigma errors in calibration.

[c] From Zimmerman and Canuel (2000).

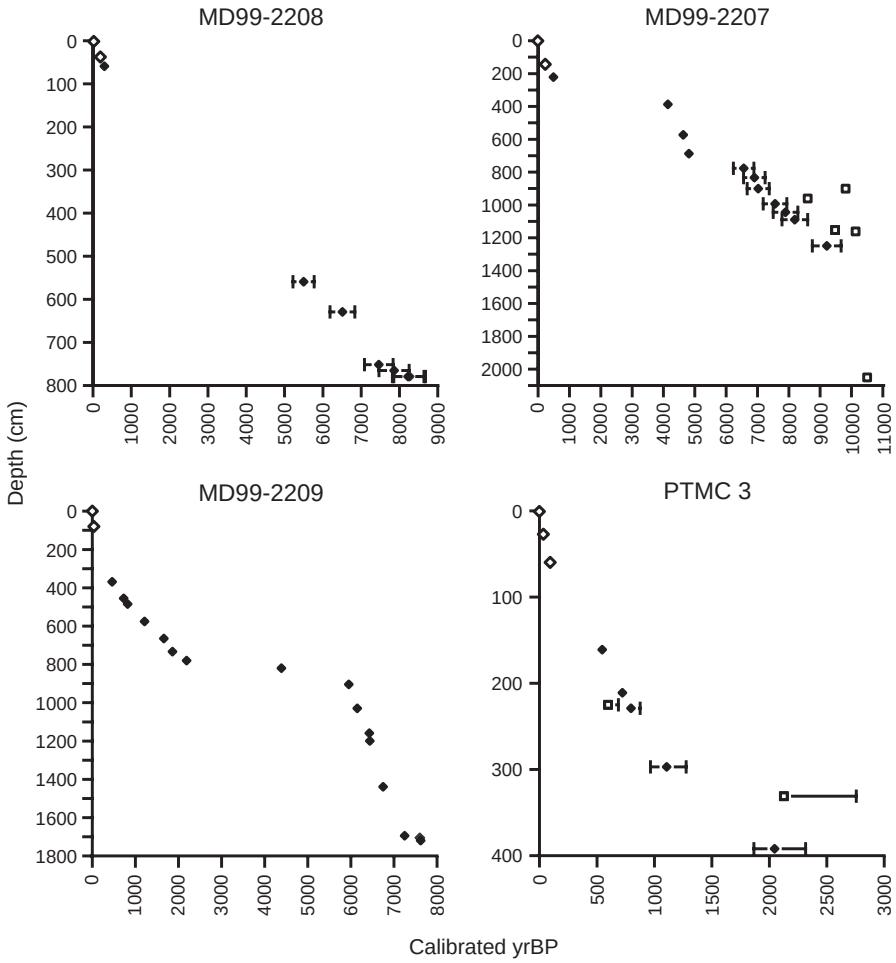

Fig. 3. Plot of calibrated radiocarbon ages against depth in cores MD00-2207, MD99-2208, and MD99-2209. Where error bars are not visible, they are smaller than the boundaries circumscribed by the size of the symbols. Diamonds represent radiocarbon dates used to develop age models; squares represent dates not used in age models because of age reversals, or $\delta^{13}C$ values that indicate transport or reworking from adjacent units. Open diamonds represent dates in the uppermost parts of the cores based on lead-210 analysis and *Ambrosia* pollen biostratigraphy. Age models for pre-Colonial (pre-1700 AD) segments of each core are as follows. MD99-2208: 59–559 cm: age=(10.398*depth)−316.482; 559–629 cm: age=(14.5008*depth)−2658.500; 629–752 cm: age=(7.739*depth)+1594.310. MD99-2207: 387–573 cm: age=(2.634*depth)+3119.167; 573–687 cm: age=(1.579*depth)+3724.474; 687–777 cm: age=(19.553*depth)− 8632.737; 777–833 cm: age=(6.018*depth)+1884.248; 833–901 cm: age=(1.852*depth)+5356.481; 901–993 cm: age=(5.815*depth)+1785.489; 993–1249 cm: age=(6.334*depth)+1159.805; 1249–2050 cm: age=(1.610*depth)+7198.502. MD99-2209: age model for upper 800 cm provided in Willard et al., 2003; 819–904 cm: age=(18.631*depth)−10937.381; 900–1200 cm: age=(1.743*depth)+4324.51; 1200–1439 cm: age=1.292*depth)+4841.292; 1439–1694 cm: age=(1.961*depth)+3878.431. PTMC 3 (160–450 cm): age=(0.012*depth2)+(0.97*depth)−41.675 (r^2=0.86).

The *Tsuga* decline at 730 cm in MD99-2207 and 840 cm in MD99-2209 is dated at 5.4 ka (Fuller, 1998). The rise in *Ambrosia* abundance at 240 cm (MD99-2209) and 160 cm (MD99-2207) represents peak land clearance at ~1880–1910 AD (Brush, 1984; Willard et al., 2003). The greatest uncertainty for these age models lies within the intervals between 2.2 ka and 4.0 ka and 5.0 ka and 5.8 ka (Fig. 3), which include

Table 2
Comparison of expected and actual radiocarbon dates on shells collected in sediments deposited between 1880 AD and 1910 AD, based on *Ambrosia* pollen biostratigraphy

Laboratory number	Core identification	Sample location	Sample depth (cm)	Material	$\delta^{13}C$ (‰)[a]	Age (^{14}C years BP)	Error[b]	Estimated pollen age[c]	Expected ^{14}C age[d]	Reservoir effect[e]
Beta 161216[f]	PC6B-2	Pocomoke Sound	202–204	*Haminoea solitaria*	−0.9	490	40	1880–1910 AD	86.5±10.8	403.5
Beta 161221[f]	PC2B-3	Pocomoke Sound	268	*Mulinia*	−0.8	460	40	1880–1910 AD	86.5±10.8	373.5
Beta 161222[f]	PC2B-3	Pocomoke Sound	380–386	*Mulinia*	−0.7	440	40	1880–1910 AD	86.5±10.8	353.5
OS 15679[g]	PTMC 3-P-2	Potomac River	80–82	*Mulinia*	0.01	540	30	1860–1900 AD	86.5±10.8	453.5
WW 1291[g]	PTXT 2-G-2	Patuxent River	85–87	*Mulinia*	0	510	60	1880–1910 AD	86.5±10.8	423.5
WW 1292[g]	PTXT 2-G-2	Patuxent River	95–97	*Mulinia*	0	520	50	1880–1910 AD	86.5±10.8	433.5
WW 2703[g]	LCPTK 1-P-3	Little Choptank River	360–362	*Mulinia*	0	460	55	1880–1910 AD	86.5±10.8	373.5
WW 2704[g]	LCPTK 1-P-3	Little Choptank River	406–408	*Mulinia*	0	540	55	1880–1910 AD	86.5±10.8	453.5
OS 19212[h]	RD 98-1	Rhode River	142	shell	−0.04	325	60	1880–1910 AD	86.5±10.8	238.5
OS 19216[h]	RD 98-1	Rhode River	203	shell	−0.4	325	60	1880–1910 AD	86.5±10.8	238.5

[a] $\delta^{13}C$ notation relative to Pee Dee Belemnite standard. Values of 0 are assumed; all others were measured.
[b] One-sigma counting error.
[c] Samples selected at depths identified as representing peak land clearance (1880–1910 AD) based on *Ambrosia* pollen abundance (see Willard et al., 2003).
[d] Expected ^{14}C age calculated as average of single-year age determinations of wood from 1880 to 1910 AD (Stuiver et al., 1998).
[e] Reservoir effect calculated as difference between ^{14}C age and average expected ^{14}C age.
[f] Dates previously published in Willard and Bernhardt (2004).
[g] Dates previously published in Cronin et al., (2000).
[h] Dates previously published in Colman et al., (2002).

either unconformities or periods of very slow deposition at these sites, with much poorer temporal resolution than in the remainder of the record.

Because no individual core represents the entire Holocene, we combined records from three cores (MD99-2207, MD99-2208, and MD99-2209) to produce a composite series representing the last 10.5 ka. To avoid the possibility of introducing an incorrect chronological order of samples by simply merging data from all four cores, we spliced together the highest resolution continuous core intervals for each time period. This resulted in omission of data from core PTMC 3 in the composite record because of temporal overlap with core MD99-2209. We also omitted samples representing the last 300 years, when Colonial land clearance and subsequent land-use practices became the primary control on plant community composition in the eastern United States. In the composite record, the average sample resolution (Δt) is 27.7 years and varies from 3 to 210 years. The most highly resolved portions of the record are from 303 to 2097 years (average Δt=37.5 years), 4139–4880 years (average Δt=12.8 years), and 5909–10,500 years (average Δt=19.1 years). This resolution permits detailed comparison of the terrestrial record of climate variability with marine records from the North Atlantic Ocean and provides an exceptionally well-resolved Holocene pollen record from eastern North America.

3.2. Methodology

Pollen was isolated from estuarine sediments using standard palynological techniques (Traverse, 1988; Willard et al., 2003). Initial sample spacing was at 10 cm, with subsequent sampling at 2 cm increments to maximize temporal resolution. For each sample, one tablet of *Lycopodium* spores was added to 5–7 g of dried sediment for calculation of pollen concentration (pollen/gram dry sediment). Samples were processed with HCl and HF to remove carbonates and silicates. Late Holocene samples (<5 ka) were acetolyzed (1 part sulphuric acid/9 parts acetic anhydride) in a boiling water bath for 10 min, neutralized, and treated with 10% KOH for 10 min in a water bath at 70 °C. Early Holocene samples (>5 ka) were treated with cold 35% nitric acid for 5 min before being heated in a boiling water bath with 10% KOH for 15 min. After neutralization, residues were sieved with 150 μm and 10 μm mesh to remove the coarse and clay fractions, respectively. When necessary, samples were swirled in a watch glass to remove mineral matter. After staining with Bismarck Brown, palynomorph residues were mounted on microscope slides in glycerin jelly. At least 300 pollen grains were counted from each sample to determine percent abundance and pollen concentration. Confidence limits for *Pinus* and *Quercus* percentages were calculated using binomial standard errors as outlined in Buzas (1990). Mann–Whitney tests were used to determine whether abundance of indicator taxa varied significantly both within and among cores. Pollen data from surface samples and sediment cores are available from the North American Pollen Database (NAPD) at the World Data Center for Paleoclimatology in Boulder, CO (http://www.ngdc.noaa.gov/paleo/pollen.html) and at the U.S. Geological Survey Atlantic Estuaries Project website (http://geology.er.usgs.gov/eespteam/Atlantic/index.htm).

3.3. Pollen records from Chesapeake Bay

Pinus and *Quercus* pollen dominate Holocene records from Chesapeake Bay sediment cores, collectively averaging 79% of pollen assemblages. *Carya* and other hardwood taxa contribute minor amounts of pollen to sediments, as do herbaceous taxa such as grasses and sedges (Fig. 4). *Quercus* is a prominent component in both oak–chestnut and oak–pine–hickory forests, and Mann–Whitney tests show that neither its percent abundance nor concentration (pollen/gram dry sediment) varied significantly before Colonial land clearance in the 17th–18th centuries. After land clearance, however, oak pollen abundance was nearly halved (Fig. 4). *Pinus*, with limited abundance and distribution in the Chesapeake Bay watershed, is characterized by significant (p<0.001, using Mann–Whitney tests) fluctuations in both percentage and concentration data between high-pine and low-pine intervals of the Holocene; decreases during low-pine intervals are greater than confidence intervals calculated for the counts (~4.5%: see Fig. 5) (Buzas, 1990).

A striking feature of Chesapeake Bay pollen records is the doubling of *Pinus* pollen between ~5.5 and 4.8 ka (Figs. 5 and 6A). The change represents the mid-Holocene shift from deciduous to mixed deciduous–conifer forests in the region. The

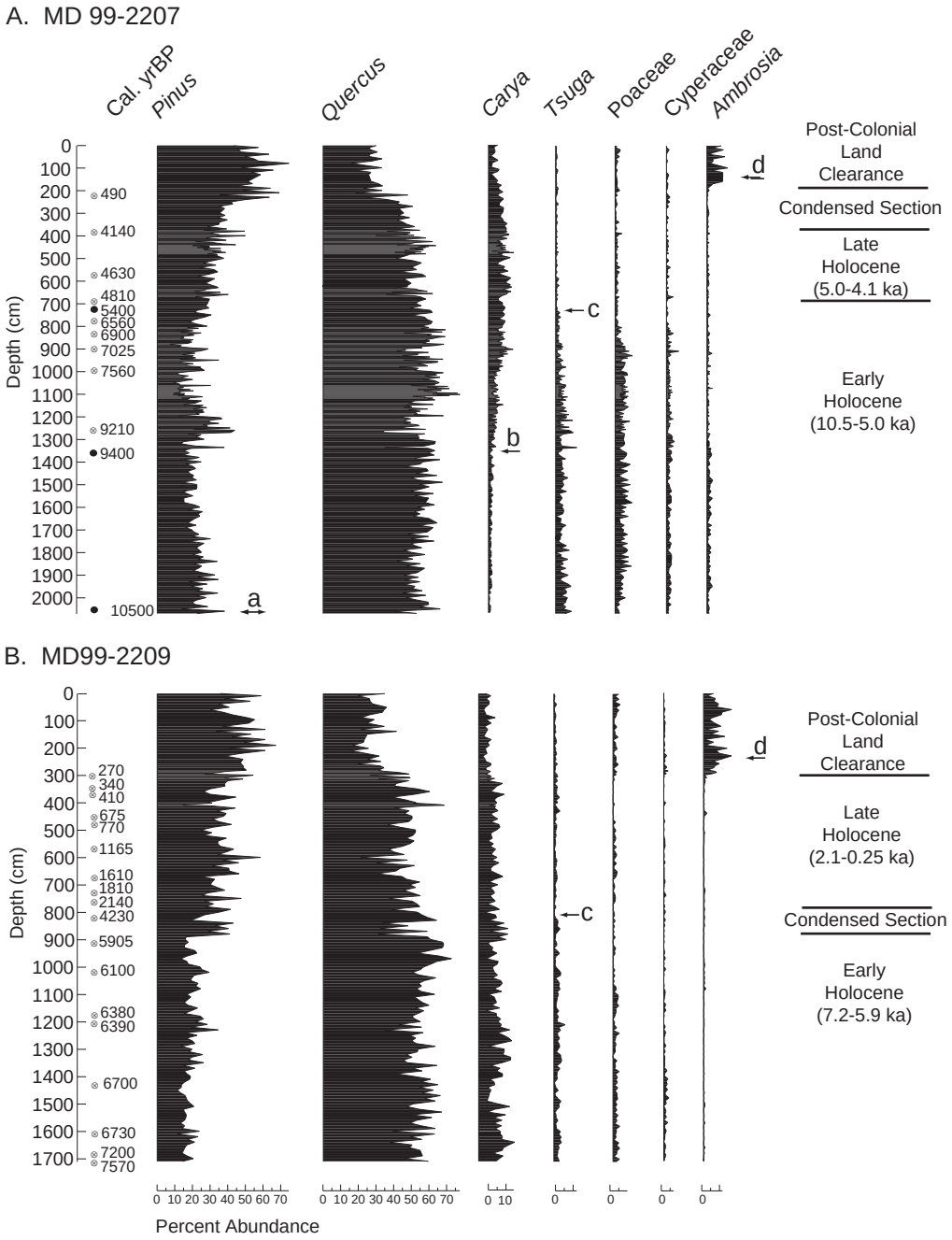

Fig. 4. Percent abundance of pollen from major plant taxa in (A) core MD99-2207 and (B) MD99-2209. Both core locations are shown in Fig. 1. Circles with "x" indicate radiocarbon dates; filled circles represent age estimates from biostratigraphic horizons (a–d). (a) *Quercus* increase ~10.5 ka; note that this is a conservative estimate and that basal sediments may be younger. (b) *Carya* increase ~9.4 ka. (c) *Tsuga* decline at 5.4 ka. (d) *Ambrosia* rise ~1880–1910 AD (see text for discussion of biostratigraphic events).

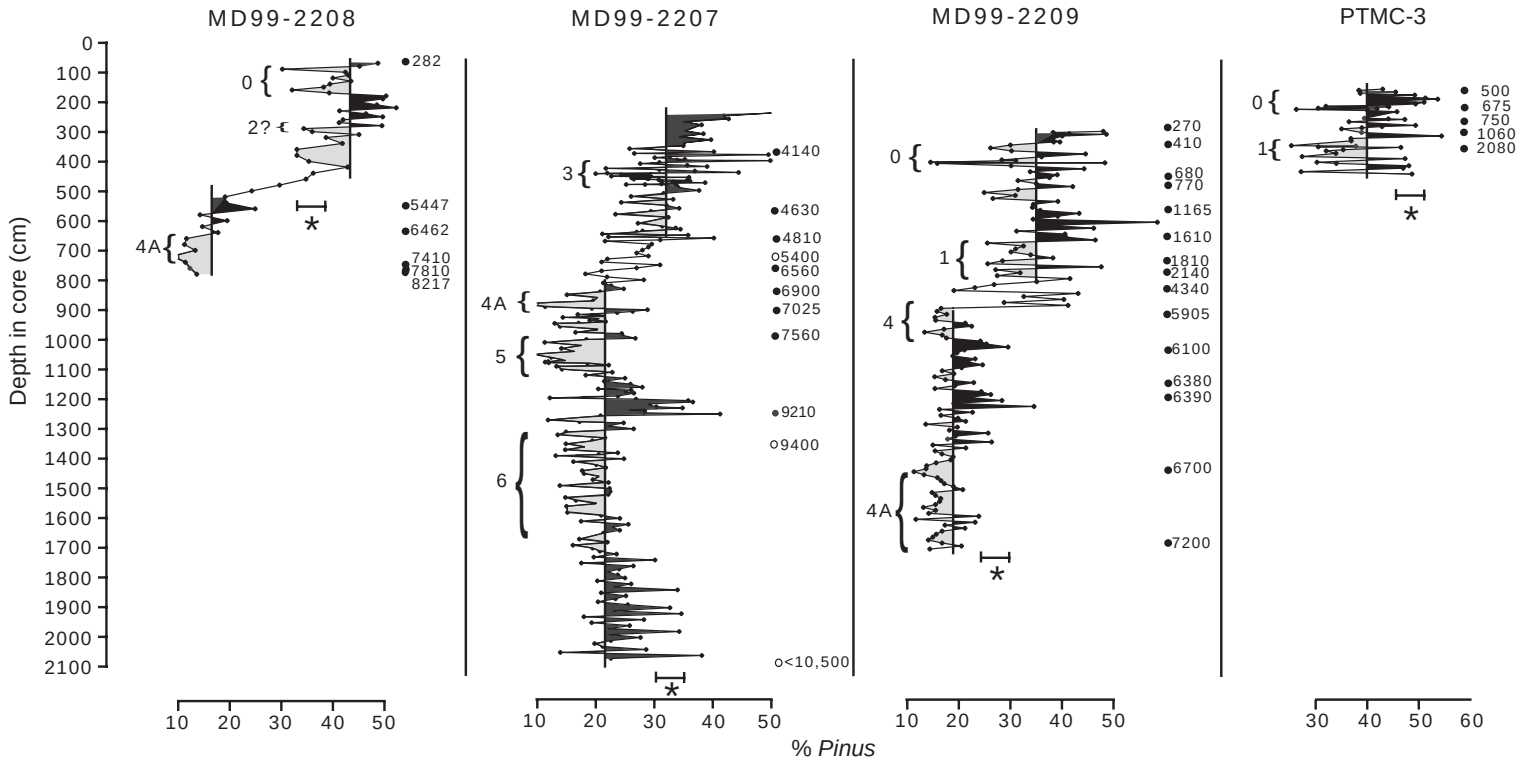

Fig. 5. Percent abundance of pine pollen vs. depth in four Chesapeake Bay cores; all core sites are indicated in Fig. 1. Vertical lines indicate early and late Holocene mean pine abundance at each site. Numbers 0–6 refer to North Atlantic millennial-scale cold events (Bond et al., 2001). Event 4A represents an additional cool event ~7 ka that was not recognized in the North Atlantic record. Black dots indicate radiocarbon dates; clear circles indicate biostratigraphic horizons. Lines with asterisks indicate the 95% confidence intervals (±4%) for the counts.

well-documented migration of southern pines along the Atlantic Coastal Plain from Florida northward to Pennsylvania and New Jersey has been attributed to warmer and wetter late Holocene winters resulting from orbitally driven solar insolation changes (Watts, 1979; Webb et al, 1987). Using temperature estimates derived from surface sample calibrations of pollen, the mid-Holocene shift corresponds to a mid-Atlantic January warming of up to 2–4 °C from the early to late Holocene. This is consistent with model reconstructions of warmer late Holocene winters due to increased winter insolation and slightly greater precipitation in eastern North America since 6 ka (Harrison et al., 2003; Kutzbach et al., 1998).

Superposed upon the mid-Holocene shift are a series of oscillations in *Pinus* abundance that suggest millennial- to centennial-scale temperature variability (Figs. 5 and 7). Multi-taper method (MTM) spectral analysis (Thomson, 1982) has been employed to quantitatively test for centennial- to millennial-scale periodic components within the composite *Pinus* abundance time series. This analysis has been restricted to the longest uninterrupted interval of high-resolution pollen data, between 5909 and 10,500 years BP, to avoid the relatively large temporal gaps (up to 210 years) in portions of the composite record (Fig. 6A). Between 5909 and 10,500 years BP, the time series is characterized by sample intervals that range from 6 to 65 years (average Δt=19.1 years, standard deviation=9.4 years); these intervals permit robust quantification of periodicities as short as 130 years (2*65 years). Following linear interpolation to an even sampling interval (5 years) and removal of a linear trend, MTM power and harmonic spectra were calculated using five 3π discrete prolate spheroidal sequence data tapers (Thomson, 1982).

MTM spectral analysis permits assessment of the variance contribution (power) at discrete frequencies in the *Pinus* abundance time series, and also provides a statistical F-test for the presence of pure sinusoidal (harmonic) components in the time series. The results of the MTM harmonic and power spectral analyses are displayed in Fig. 6. The harmonic analysis results indicate five highly significant (>90% significance) periodic components in the centennial–millennial band: 1429, 521, 282, 177, and 148 years (Fig. 6C, gray spectrum). The 1429-year periodic component displays the greatest amplitude (Fig. 6C, bold line), and the power spectrum (Fig. 6B, bold line) indicates that variability within the millennial band is the dominant source of variance in this portion of the *Pinus* abundance record. Relatively high power is also associated with the significant periodic components identified at 282 and 148 years.

Millennial-scale periodic variability in the entire Holocene time series is expressed as relatively prolonged minima in *Pinus* abundance (events numbered 0–6 in Fig. 7). These minima are clearly observed following smoothing with a 400-year moving average (Fig. 7A), and in lowpass-filtered versions of the *Pinus* abundance record (Fig. 7B). The spacing of the centers of the minima is not precisely 1429 years, but varies due to interference between the identified periodic components, inaccuracies in the time model, additional non-periodic noise in the climate proxy record, and/or temporal variability in the millennial-scale periodic forcing. Because southern pine distribution is limited primarily by winter temperature, we interpret these sustained *Pinus* minima as cooler, drier intervals in which January temperature decreased by 0.2° to 2 °C, resulting in minor decreases in *Pinus* abundance in adjacent forests.

Several of the Holocene pine minima are noteworthy. Events 6 and 5 (centered at 9.5 and 8.1 ka, respectively) are preserved in freshwater sediments deposited in the channel of the paleo-Susquehanna River before formation of the Chesapeake Bay estuary by sea-level rise ~7.6 ka. Rapid mean sedimentation rates in this interval (~0.36 cm year^{-1}) resulted in high temporal resolution. The termination of Event 5 coincides with a shift from fresh to brackish conditions associated with the final stages of sea-level rise associated with Laurentide and Antarctic ice sheet decay (Berke and Cronin, 2004; Vogt et al., 2000). In the pollen record the corresponding decrease in riverbank/marsh herb abundance (Cyperaceae, Poaceae) (Fig. 4) represents the impact of transgression across the paleo-Susquehanna shoreline. Flooding of the original river channel to form the much wider bay submerged the original shoreline marshes. The greater distance from the subsequent shoreline to the core site apparently was too great for effective transport of marsh plant pollen to the site, minimizing their representation in pollen assemblages.

Event 5, lasting from ~8.3 ka to ~8.0 ka, corresponds to a widespread cool event centered at

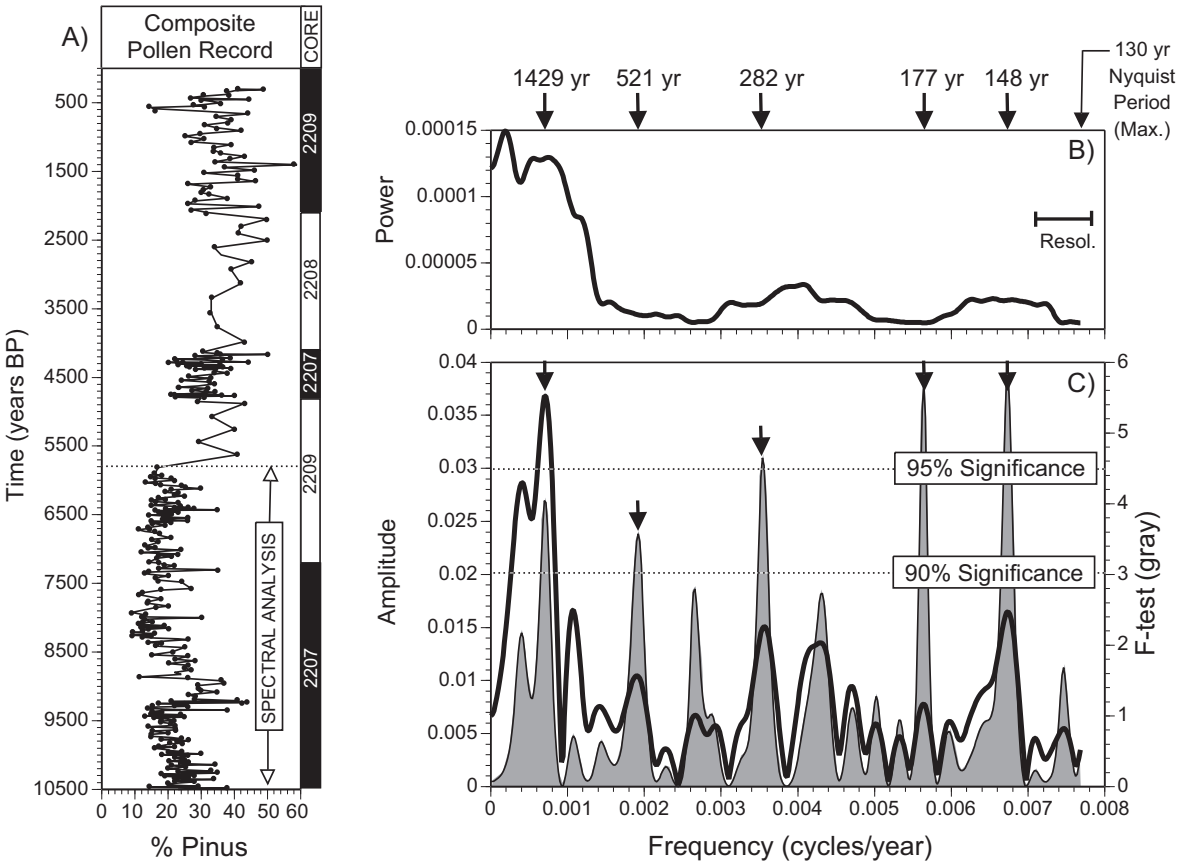

Fig. 6. (A) Composite record of % *Pinus* pollen from three CB cores (MD99-2207, MD99-2208, MD99-2209). The spacing between solid dots reflects the variable sampling resolution of the composite record. (B) MTM power spectrum for the composite record from 5909 to 10,500 years BP, employing five $3\frac{1}{4}$ discrete prolate spheroidal sequence data tapers. (C) MTM harmonic analysis results for the composite record from 5909 to 10,500 years BP, employing five $3\frac{1}{4}$ discrete prolate spheroidal sequence data tapers. Amplitude is plotted as a bold line, and the *F*-test results are indicated in gray. 90% and 95% significance levels for the *F*-test results are indicated as dotted lines.

8.2 ka, in which high-latitude temperatures dropped 4–8 °C and marine and terrestrial sites cooled by 1.5–3 °C (Alley et al., 1997; Barber et al., 1999). Using the pine–temperature correlation in Fig. 2, Chesapeake Bay pollen data suggest a decrease in atmospheric January temperature of up to 3 °C in the mid-Atlantic United States. Proxy evidence and model results indicate that the primary driver of this event was a rapid meltwater release associated with collapse of the Laurentide ice sheet (Barber et al., 1999; von Grafenstein et al., 1998; Renssen et al., 2001), but ^{14}C and ^{10}Be records also indicate a concomitant solar

Fig. 7. Composite record of pine pollen abundance from three CB cores (MD99-2207, -2208, -2209) compared with Dec. insolation record (30°N) (Berger and Loutre, 1991) and ^{14}C record from GISP2 ice core (Bond et al., 2001). In (A), pine abundance is illustrated by a black line, and a 400-year moving average is superimposed in red. The insolation curve is shown by the dashed black line. In (B), the red line illustrates results of a lowpass filtering of the composite % *Pinus* record. Data filtering employed a 20% cosine window, with cutoff frequencies of 1000 years (thick line) and 500 years (thin line). A linear trend was removed from the composite % *Pinus* record prior to lowpass filtering. The GISP2 ice-core record of ^{14}C is shown in black. Gray boxes indicate the duration of cool mid-Atlantic climate; associated numbers indicate North Atlantic ice-rafting events (Bond et al., 1999, 2001). The timing of Greenland cold intervals (Johnsen et al., 2001), times of polar cell expansion (O'Brien et al., 1995), glacial advances (Denton and Karlen, 1973), and cooler sub-tropical Atlantic sea-surface temperatures (deMenocal et al., 2000) are shown by bars.

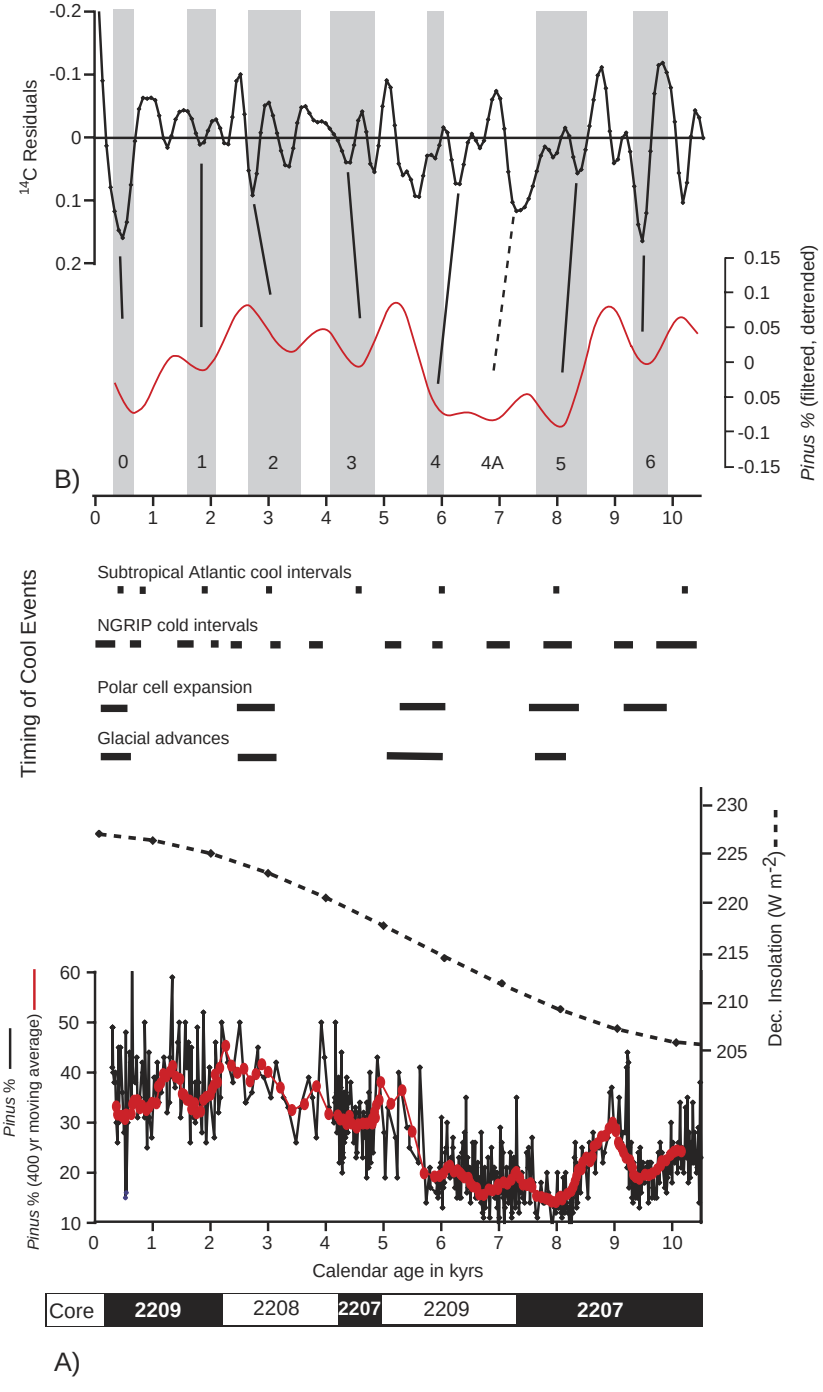
^{14}C Residuals
-0.2
-0.1
0
0.1
0.2
0
1
2
3
4
4A
5
6
B)
0 1 2 3 4 5 6 7 8 9 10
0.15
0.1
0.05
0
0.05
-0.1
-0.15
Pinus % (filtered, detrended)
Timing of Cool Events
Subtropical Atlantic cool intervals
NGRIP cold intervals
Polar cell expansion
Glacial advances
230
225
220
215
210
205
Dec. Insolation (W m^{-2})
Pinus %
Pinus % (400 yr moving average)
60
50
40
30
20
10
0 1 2 3 4 5 6 7 8 9 10
Calendar age in kyrs
Core
2209
2208
2207
2209
2207
A)

minimum (Bond et al., 2001). The large decrease in abundance of pine pollen during this time probably represents the paired impacts of cooler temperatures and drier, windier conditions documented from high-latitude sites (Alley et al., 1997) and the mid-continent United States (Hu et al., 1999).

Another pine minimum centered at 1.8 ka (Event 1) corresponds to relatively cooler spring conditions in Chesapeake Bay, documented by Mg/Ca ratios from foraminiferal shells (Cronin et al., 2003). The most recent pine minimum associated with the Little Ice Age (LIA: Event 0) cooling represents a two-step event (Fig. 5), with the first, more severe, minimum between 650 years BP and 550 years BP and the second between 450 years BP and 350 years BP. During the LIA cooling events, Chesapeake Bay waters cooled by 2–4 °C (Cronin et al., 2003), and ice-rafted debris were more abundant in the North Atlantic Ocean (Bond et al., 1999). Because land clearance began early in the 17th century and was well-established by 1750 AD, the subsequent warming after the LIA is obscured in pollen records by anthropogenic changes to the regional vegetation.

4. Correlation of terrestrial and marine records

The approximate 1400-year periodicity of mid-Atlantic pine minima/cool intervals is similar to periodicities of cold intervals in the North Atlantic identified using petrographic indicators (Bond et al., 2001), $\delta^{18}O$ records of cooler conditions and/or changes in atmospheric circulation interpreted from the NGRIP ice core and from Irish speleothems (Johnsen et al., 2001; McDermott et al., 2001), foraminiferal evidence for cooling in the sub-tropical Atlantic Ocean (deMenocal et al., 2000), sea-salt (K) records of increased aridity from the GISP2 ice core (O'Brien et al., 1995), and biological and geochemical records from southwestern Alaska (Hu et al., 2003), even with the inherent limitations of chronological comparisons among different records (Fig. 7). The correlations are poorest between ~2.2 ka and 4 ka and 5 ka and 5.8 ka, when sedimentation rates were slow or where unconformities exist in these Chesapeake Bay cores. In the early and late Holocene, however, the peaks and troughs match extremely well, and the quasi-periodicity of ~1400 years is comparable to the pattern shown by North Atlantic drift-ice records (Bond et al., 1997, 1999, 2001).

The North Atlantic Holocene cold cycles have been linked in unknown ways to solar variability through comparison with cosmogenic isotope records (Bond et al., 2001). A potential explanation for millennial-scale patterns observed in Holocene proxy records lies in the relationship between solar wind strength and large-scale, atmospheric pressure systems on earth over decadal to centennial time scales (Angell, 1998; Boberg and Lundstedt, 2002; Tinsley, 2000; Tinsley and Heelis, 1993). Solar wind strength has been linked to cloudiness, configuration of the circumpolar vortex and planetary waves, and to latitudinal shifts of storm tracks across the North Atlantic Ocean documented between sunspot maxima and minima (Tinsley, 2000). Solar maxima have been correlated with increased Northern Hemisphere land temperature (1861–1989 AD) and decreased sea-ice extent around Iceland (1740–1970 AD) (Friis-Christensen and Lassen, 1991). Likewise, using general circulation models, Shindell et al. (2001) showed that reduced solar irradiance during the late 17th century Maunder Minimum altered atmospheric circulation patterns in the North Atlantic region, resulting in colder winters over northern hemisphere continents. Such results are consistent with the hypothesis that solar variability directly influences atmospheric circulation patterns and climate on a global scale over a variety of time scales.

The similar periodicities exhibited by Chesapeake Bay pine minima and cosmogenic isotope (^{10}Be and ^{14}C) maxima (Fig. 7B), indicating low solar activity, suggest long-term, possibly solar-driven shifts toward a periodically expanded circumpolar vortex and altered jet stream. Intervals of increased Holocene Arctic storminess and aridity (Mayewski et al., 1997) and altered eastern European lake levels (Magny et al., 2002) have similar periodicities to the Chesapeake Bay record and have been attributed to fluctuating polar cell size and resultant changes in the jet stream. The hypothesis of periodic, long-term solar minima catalyzing extended intervals of circumpolar vortex expansion and enhanced meridionality could explain why no synchronous, ubiquitous cooling responses have been documented in response to decreased solar activity during observed millennial-scale year cycles (Rind, 2002). Changes in the configuration of the

planetary wave pattern are manifested by regional differences in climate rather than a globally uniform response (Davis and Benkovic, 1992). Other forcing factors also may amplify or dampen the regional response to solar variability. For example, although long-term records of vulcanism from ice cores do not share the observed ~1400 periodicity, extensive vulcanism between 7 and 9 ka and during the Little Ice Age (Zielinski et al., 1994) may have augmented climatic extremes related to solar minima. Changes in oceanic thermohaline circulation (Bond et al., 2001) also may be related to changes in atmospheric circulation. As additional terrestrial and marine records exhibiting similar periodicities are developed, it should be possible to better understand the relative influence of solar variability on global, long-term atmospheric circulation patterns and compare it to other external factors influencing these millennial-scale events.

Acknowledgements

We thank the crew and scientific staff of the R/V *Marion Dufresne* and the IMAGES V program for providing cores MD99-2207, -2208, and -2209 and for other assistance with the cruise. We also thank Rick Younger and the crew of the R/V *Kerhin* for assistance in piston coring. Cheryl Vann provided assistance with statistical analyses. We acknowledge helpful discussions with Gerard Bond and Thomas Cronin during the course of the research. Chris Swezey, Blaine Cecil, and Dorothy Peteet provided helpful comments on earlier versions of the manuscript. We thank Stephen Pekar and an anonymous reviewer for subsequent reviews of the manuscript. We acknowledge the laboratory and field assistance of P. Buchanan, J. Damon, A. Fagenholtz, J. Murray, T. Sheehan, N. Waibel, and L. Weimer. This research was supported by the U.S. Geological Survey Earth Surface Dynamics and Priority Ecosystem Studies Programs.

References

Alley, R.B., Mayewski, P.A., Sowers, T., Stuiver, M., Taylor, K.C., Clark, P.U., 1997. Holocene climatic instability: a prominent, widespread event 8200 yr ago. Geology 25, 483–486.

Angell, J.K., 1992. Relation between 300-mb north polar vortex and equatorial SST, QBO, and sunspot number and the record contraction of the vortex in 1988–89. Journal of Climate 5, 22–29.

Angell, J.K., 1998. Contraction of the 300 mbar north circumpolar vortex during 1963–1997 and its movements into the eastern hemisphere. Journal of Geophysical Research 103, 25,887–25,893.

Barber, D.C., Dyke, A., Hillaire-Marcel, C., Jennings, A.E., Andrews, J.T., Kerwin, M.W., Bilodeau, G., McNeely, R., Southon, J., Morehead, M.D., Gagnon, J.-M., 1999. Forcing of the cold event of 8,200 years ago by catastrophic drainage of Laurentide lakes. Nature 400, 344–348.

Bartlein, P.J., Prentice, I.C., Webb III, T., 1986. Climatic response surfaces from pollen data for some eastern North American taxa. Journal of Biogeography 13, 35–57.

Berger, A., Loutre, M.F., 1991. Insolation values for the climate of the last 10 million years. Quarternary Science Reviews 10, 297–317.

Berke, M.A., Cronin, T.M., 2004. Early holocene marsh foraminifera and ostracodes from Chesapeake Bay: implications for sea-level history. Geological Society of America Abstracts with Programs 36 (5), 293.

Boberg, F., Lundstedt, H., 2002. Solar wind variations related to fluctuations of the North Atlantic Oscillation. Geophysical Research Letters 29 (15).

Bond, G.C., Showers, W., Cheseby, M., Lotti, R., Almasi, P., deMenocal, P., Priore, P., Cullen, H., Hajdas, I., Bonani, G., 1997. A pervasive millennial-scale cycle in North Atlantic Holocene and Glacial climates. Science 278, 1257–1266.

Bond, G.C., Showers, W., Elliot, M., Evans, M., Lotti, R., Hajdas, I., Bonani, G., Johnsen, S., 1999. The North Atlantic's 1–2 kyr climate rhythm: relation to Heinrich events, Dansgaard/Oeschger cycles and the Little Ice Age. In: Clark, P., Webb, R., Keigwin, L.D. (Eds.), Mechanisms of Global Climate Change at Millennial Time Scales, Geophysical Monograph Series, vol. 112, pp. 35–58.

Bond, G.C., Kromer, B., Beer, J., Muscheler, R., Evans, M.N., Showers, W., Hoffmann, S., Lotti-Bond, R., Hajdas, I., Bonani, G., 2001. Persistent solar influence on North Atlantic climate during the Holocene. Science 294, 2130–2136.

Braun, E.L., 1950. Deciduous Forests of Eastern North America. The Blakiston, Philadelphia.

Brush, G.S., 1984. Patterns of recent sediment accumulation in Chesapeake Bay (VA, MD, U.S.A.) tributaries. Chemical Geology 44, 227–242.

Brush, G.S., Lenk, C., Smith, J., 1980. The natural forests of Maryland: an explanation of the vegetation map of Maryland. Ecological Monographs 50, 77–92.

Buening, K.R.M., Fransen, L., Nakityo, B., Mecray, E.L., Buchholtz ten Brink, M.R., 2000. Modern pollen deposition in Long Island Sound. Journal of Coastal Research 16, 656–662.

Buzas, M.A., 1990. Another look at confidence limits for species proportions. Journal of Paleontology 64, 842–843.

Colman, S.M., Halka, J.P., 1989. Maps showing Quaternary geology of the southern Maryland part of the Chesapeake Bay. U.S. Geological Survey Miscellaneous Field Studies Map 1948C.

Colman, S.M., Baucom, P., Bratton, J.F., Cronin, T.M., McGeehin, J.P., Willard, D., Zimmerman, A.R., Vogt, P.R., 2002. Radiocarbon dating, chronologic framework, and changes in accumulation rates of Holocene estuarine sediments from Chesapeake Bay. Quaternary Research 57, 58–70.

Cronin, T.M., Willard, D., Karlsen, A., Ishman, S., Verardo, S., McGeehin, J., Kerhin, R., Holmes, C., Zimmerman, A., 2000. Climatic variability in the eastern United States over the past millennium from Chesapeake Bay sediments. Geology 28, 3–6.

Cronin, T.M., Dwyer, G.S., Kamiya, T., Schwede, S., Willard, D.A., 2003. Medieval Warm Period, Little Ice Age and 20th century temperature variability from Chesapeake Bay. Global and Planetary Change 36, 17–29.

Davis, R.E., Benkovic, S.R., 1992. Climatological variations in the Northern Hemisphere circumpolar vortex in January. Theoretical and Applied Climatology 46, 63–73.

deMenocal, P., Ortiz, J., Guilderson, T., Sarnthein, M., 2000. Coherent high- and low-latitude climate variability during the Holocene warm period. Science 288, 2198–2202.

Denton, G.H., Karlen, W., 1973. Holocene climate variations their pattern and possible causes. Quarternary Research 3, 155–205.

Edwards, L.E., Willard, D.A., 2001. Dinoflagellate cysts and pollen from sediment samples, Mississippi Sound and Gulf of Mexico. In: Gohn, G.S. (Ed.), Stratigraphic Framework of the Neogene and Quaternary Sediments of the Mississippi Coastal Zone, Jackson County, Mississippi. U.S. Geological Survey Open-file Report 01-415 (CD-ROM).

Emery, K.O., 1966. Atlantic continental shelf and slope of the United States. U.S. Geological Survey Professional Paper 529-A, 1–23 pp.

Friis-Christensen, E., Lassen, K., 1991. Length of the solar cycle: an indicator of solar activity closely associated with climate. Science 254, 698–700.

Fuller, J.L., 1998. Ecological impact of the mid-Holocene hemlock decline in southern Ontario, Canada. Ecology 79, 2337–2351.

Greller, A.M., 1988. Deciduous forest. In: Barbour, M.G., Billings, W.D. (Eds.), North American Terrestrial Vegetation. Cambridge University Press, Cambridge, pp. 288–316.

Halka, J.P., Vogt, P.R., Czarnecki, M., 2000. Marion-Dufresne coring in Chesapeake Bay: geophysical environment at sites MD99-2204 and 2207. In: Cronin, T.M. (Ed.), Initial Report on IMAGES V Cruise of the Marion-Dufresne to Chesapeake Bay June 20–22, 1999, pp. 40–48. U.S. Geological Survey Open-File Report 00-306.

Harrison, S.P., Kutzbach, J.E., Liu, Z., Bartlein, P.J., Otto-Bliesner, B., Muhs, D., Prentice, I.C., Thompson, R.S., 2003. Mid-Holocene climates of the Americas: a dynamical response to changed seasonality. Climate Dynamics 20, 663–688.

Hobbs III, C.H., 2004. Geological history of Chesapeake Bay, USA. Quaternary Science Reviews 23, 641–661.

Hu, F.S., Slawinski, D., Wright Jr., H.E., Ito, E., Johnson, R.G., Kelts, K.R., McEwan, R.F., Boedigheimer, A., 1999. Abrupt changes in North American climate during early Holocene times. Nature 400, 437–440.

Hu, F.S., Kaufman, D., Yoneji, S., Nelson, D., Shemesh, A., Huang, Y., Tian, J., Bond, G., Clegg, B., Brown, T., 2003. Cyclic variation and solar forcing of Holocene climate in the Alaskan subarctic. Science 301, 1890–1893.

Iverson, L.R., Prasad, A.M., Hale, B.J., Sutherland, E.K., 1999. Atlas of current and potential future distributions of common trees of the Eastern United States. USDA Forest Service General Technical Report, NE-265.

Johnsen, S.J., Dahl-Jensen, D., Gundestrup, N., Steffensen, J.P., Clausen, H.B., Miller, H., Masson-Delmotte, V., Sveinbjörnsdottir, A.E., White, J., 2001. Oxygen isotope and palaeotemperature records from six Greenland ice-core stations: camp century, Dye-3, GRIP, SIGP2, Renland, and NorthGRIP. Journal of Quaternary Science 16, 299–307.

Keigwin, L.D., Pickart, R.S., 1999. Slope water current over the Laurentian fan on interannual to millennial time scales. Science 286, 520–523.

Kneller, M., Peteet, D., 1993. Late-Quaternary climate in the ridge and valley of Virginia, U.S.A.: changes in vegetation and depositional environment. Quaternary Science Reviews 12, 613–628.

Kutzbach, J.E., Gallimore, R., Harrison, S., Behling, P., Selin, R., Laarif, F., 1998. Climate and biome simulations for the past 21,000 years. Quaternary Science Reviews 17, 473–506.

Litwin, R.J., Andrle, V.A.S., 1992. Modern palynomorph and weather census data from the U.S. Atlantic coast (Continental Margin Program samples and selected NOAA weather stations). U.S. Geological Survey Open-file Report 92-263, 1-31.

Magny, M.A., Miramont, C., Sivan, O., 2002. Assessment of the impact of climate and anthropogenic factors on Holocene Mediterranean vegetation in Europe on the basis of palaeohydrological records. Palaeogeography, Palaeoclimatology, Palaeoecology 197, 47–59.

Mayewski, P.A., Meeker, L.D., Twickler, M.S., Whitlow, S., Yan, Q., Lyons, W.B., Prentice, M., 1997. Major features and forcing of high-latitude northern hemisphere atmospheric circulation using a 110,000-year-long glaciochemical series. Journal of Geophysical Research 102, 26,345–26,366.

McDermott, F., Mattey, D.P., Hawkesworth, C., 2001. Centennial-scale Holocene climate variability revealed by a high-resolution speleothem $\delta^{18}O$ record from SW Ireland. Science 294, 1328–1331.

Mudie, P.J., 1980. Palynology of later Quaternary marine sediments, eastern Canada. PhD thesis. Dalhousie University, Halifax, Nova Scotia.

Mudie, P.J., 1982. Pollen distribution in recent marine sediments, eastern Canada. Canadian Journal of Earth Sciences 19, 729–747.

National Climatic Data Center, Climate Atlas of the United States. CD-ROM Disk 1 (Sept., 2000).

O'Brien, S.R., Mayewski, P.A., Meeker, L.D., Meese, D.A., Twickler, M.S., Whitlow, S.I., 1995. Complexity of Holocene climate as reconstructed from a Greenland ice core. Science 270, 1962–1964.

Pang, K., Yau, K.K., 2002. Ancient observations link changes in sun's brightness and earth's climate. EOS, Transactions, American Geophysical Union 481, 489–490.

Renssen, H., Goosse, H., Fichefet, T., Campin, J.-M., 2001. The 8.2 kyr BP event simulated by a global atmosphere–sea-ice–ocean model. Geophysical Research Letters 28, 1567–1570.

Rind, D., 2002. The sun's role in climate variations. Science 296, 673–677.

Shindell, D.T., Schmidt, G.A., Mann, M.E., Rind, D., Waple, A., 2001. Solar forcing of regional climate change during the Maunder Minimum. Science 294, 2149–2152.

Smith, W.B., Vissage, J.S., Darr, D.R., Sheffield, R.M., 1997. Forest resources of the United States, 1997. United States Department of Agriculture Forest Service General Technical Report NC-219, 1–198.

Stuiver, M., Reimer, P.J., Braziunas, T.F., 1998. High-precision radiocarbon age calibration for terrestrial and marine samples. Radiocarbon 40, 1127–1151.

Thompson, R.S., Anderson, K.H., Bartlein, P.J., 2000. Atlas of relations between climatic parameters and distributions of important trees and shrubs in North America—Introduction and conifers. U.S. Geological Survey Professional Paper 1650-A, 1–269.

Thomson, D.J., 1982. Spectrum estimation and harmonic analysis. IEEE Proceedings 70, 1055–1096.

Tinsley, B.A., 2000. Influence of solar wind on the global electric circuit, and inferred effects on cloud microphysics, temperature, and dynamics in the troposphere. Space Science Reviews 94, 231–258.

Tinsley, B.A., Heelis, R.A., 1993. Correlations of atmospheric dynamics with solar activity: evidence for a connection via the solar wind, atmospheric electricity, and cloud microphysics. Journal of Geophysical Research 98, 10,375–10,384.

Traverse, A., 1988. Paleopalynology. Unwin-Hyman, Boston.

Vega, A.J., Sui, C.H., Lau, K.M., 1998. Interannual to interdecadal variations of the regionalized surface climate of the United States and relationships to generalized flow parameters. Physical Geography 19, 271–291.

Vega, A.J., Rohli, R.V., Sui, C.H., 1999. Climatic relationships to Chesapeake Bay salinity during Southern Oscillation extremes. Physical Geography 20, 468–490.

Vogt, P.R., Czarnecki, M., Halka, J.P., 2000. Marion-Dufresne coring in Chesapeake Bay, geophysical environment at sites MD99-2204 and 2207. In: Cronin, T.M. (Ed.), Initial Report on IMAGES V Cruise of the Marion Dufresne to Chesapeake Bay June 20–22, 1999, pp. 32–39. U.S. Geological Survey Open-File Report 00-306.

von Grafenstein, U., Erlenkeuser, H., Müller, J., Jouzel, J., Johnsen, S., 1998. The cold event 8200 years ago documented in oxygen isotope records of precipitation in Europe and Greenland. Climate Dynamics 14, 73–81.

Watts, W.A., 1979. Late Quaternary vegetation of central Appalachia and the New Jersey coastal plain. Ecological Monographs 49, 427–469.

Webb III, T., Bartlein, P.J., Kutzbach, J.E., 1987. Climatic change in eastern North America during the past 18,000 years; comparisons of pollen data with model results. In: Ruddiman, W.R., Wright Jr., H.E. (Eds.), North America and Adjacent Oceans During the last Deglaciation. Geological Society of America, Boulder, Colorado, pp. 447–462.

Willard, D.A., 1994. Palynological record from the North Atlantic region at 3 Ma: vegetational distribution during a period of global warmth. Review of Palaeobotany and Palynology 83, 275–297.

Willard, D.A., Bernhardt, C.E., 2004. Pollen stratigraphy and land-use change, Pocomoke Sound, Maryland. In: Cronin, T.M. (Ed.), Pocomoke Sound Sedimentary and Ecosystem History. U.S. Geological Survey Open-File Report 2004-1350.

Willard, D.A., Cronin, T.M., Verardo, S., 2003. Late-Holocene climate and ecosystem history from Chesapeake Bay sediment cores, USA. The Holocene 13, 201–214.

Willett, H.C., 1949. Long-period fluctuations of the general circulation of the atmosphere. Journal of Meteorology 6, 34–50.

Zielinski, G.A., Mayewski, P.A., Meeker, L.D., Whitlow, S., Twickler, M.S., Morrison, M., Meese, D., Alley, R., Gow, A.J., 1994. Record of volcanism since 7000 B.C. from the GISP2 Greenland ice core and implications for the volcano-climate system. Science 264, 948–952.

Zimmerman, A.R., Canuel, E.A., 2000. A geochemical record of eutrophication and anoxia in Chesapeake Bay sediments: anthropogenic influence on organic matter composition. Marine Chemistry 69, 117–137.